Connexin26 Mutations Causing Palmoplantar Keratoderma and Deafness Interact with Connexin43, Modifying Gap Junction and Hemichannel Properties

Zunaira Shuja[1,2], Leping Li[1], Shashank Gupta[3], Gülistan Meşe[4] and Thomas W. White[1]

Mutations in *GJB2* (connexin [Cx]26) cause either deafness or deafness associated with skin diseases. That different disorders can be caused by distinct mutations within the same gene suggests that unique channel activities are influenced by each class of mutation. We have examined the functional characteristics of two human mutations, Cx26-H73R and Cx26-S183F, causing palmoplantar keratoderma (PPK) and deafness. Both failed to form gap junction channels or hemichannels when expressed alone. Coexpression of the mutants with wild-type Cx43 showed a transdominant inhibition of Cx43 gap junction channels, without reductions in Cx43 protein synthesis. In addition, the presence of mutant Cx26 shifted Cx43 channel gating and kinetics toward a more Cx26-like behavior. Coimmunoprecipitation showed Cx43 being pulled down more efficiently with mutant Cx26 than wild-type, confirming the enhanced formation of heteromeric connexons. Finally, the formation of heteromeric connexons resulted in significantly increased Cx43 hemichannel activity in the presence of Cx26 mutants. These findings suggest a common mechanism whereby Cx26 mutations causing PPK and deafness transdominantly influence multiple functions of wild-type Cx43. They also implicate a role for aberrant hemichannel activity in the pathogenesis of PPK and further highlight an emerging role for Cx43 in genetic skin diseases.

Journal of Investigative Dermatology (2016) **136,** 225-235; doi:10.1038/JID.2015.389

INTRODUCTION

Gap junctions form intercellular channels between adjacent cells (Goodenough and Paul, 2003). The oligomerization of six connexins results in half of a gap junction channel referred to as a hemichannel. Connexins allow small metabolites to flow between cells (Bevans et al., 1998; Kanno and Loewenstein, 1964; Lawrence et al., 1978; Veenstra, 1996), and their disruption results in deleterious phenotypes in tissues like the cochlea and epidermis (Brissette et al., 1994; Caputo and Peluchetti, 1977; Zhao et al., 2006).

The basal layer of the epidermis contains proliferating keratinocytes, whose differentiation produces an outward migration of cells into the spinous and granular layers (Blanpain and Fuchs, 2006, 2009). Keratinocytes have many intercellular connections, including gap junctions (Kam et al., 1986). Connexins are expressed in the epidermis and the most prominent is connexin (Cx)43, which is found throughout the basal, spinous, and granular layers (Butterweck et al., 1994; Di et al., 2001; Goliger et al., 1996; Guo et al., 1992; Risek et al., 1992; Salomon et al., 1994; Wiszniewski et al., 2000).

Mutations in *GJB2*, encoding Cx26, result in syndromic skin diseases including palmoplantar keratoderma (PPK) with deafness, Vohwinkel syndrome, and keratitis-ichthyosis-deafness syndrome (KID) (Bakirtzis et al., 2003; de Zwart-Storm et al., 2011a, 2011b; Richard et al., 2004; van Steensel, 2004; Zelante et al., 1997). KID syndrome comprises vascularizing keratitis, deafness, hair follicle deficiencies, and erythrokeratoderma. Patients have repeated cutaneous infections that can produce lethal septicemia (Griffith et al., 2006; Janecke et al., 2005; Jonard et al., 2008) and an increased risk of squamous cell carcinoma (Mazereeuw-Hautier et al., 2007). In contrast, the skin phenotype of PPK associated with deafness is largely limited to hyperkeratosis of the palms and soles (Richard et al., 1998; Rouan et al., 2001). Vohwinkel syndrome is similar to PPK but includes constriction bands on the digits (pseudoainhum) leading to autoamputation (Maestrini et al., 1999). The mechanism whereby Cx26 mutations result in KID syndrome has been studied extensively (Lee and White, 2009); however, a conclusive determination has yet to be reached for mutations associated with PPK.

We examined functional attributes of two Cx26 mutations associated with PPK, Cx26-H73R, and Cx26-S183F (de Zwart-Storm et al., 2008a, 2008b). We observed a lack of gap junction channel or hemichannel formation by these

[1]*Department of Physiology and Biophysics, Stony Brook University, Stony Brook, New York, USA;* [2]*Graduate Program in Genetics, Stony Brook University, Stony Brook, New York, USA;* [3]*InSTAR Program, Ward Melville High School, Setauket, New York, USA; and* [4]*Department of Molecular Biology and Genetics, Izmir Institute of Technology, Urla, Izmir, Turkey*

Correspondence: Thomas W. White, Department of Physiology and Biophysics, Stony Brook University, T5-147 Basic Science Tower, Stony Brook, NY 11794-8661. E-mail: thomas.white@stonybrook.edu

Abbreviations: Cx26, connexin26; Cx43, connexin43; G_j, gap junctional conductance; I_j, junctional currents; KHLS, keratoderma-hypotrichosis-leukonychia totalis syndrome; KID, keratitis-ichthyosis-deafness; PPK, palmoplantar keratoderma; V_j, transjunctional potentials

Received 23 April 2015; revised 3 September 2015; accepted 21 September 2015; accepted manuscript published online 6 October 2015

mutations when expressed alone yet revealed an ability of these mutations to modify the functional activity of and associate with Cx43. Furthermore, we observed changes in hemichannel activity and voltage gating due to interactions of Cx43 with mutant proteins. These observations suggest that some syndromic deafness mutations in Cx26 exert their pathologic effects through dominant gains of function and suggest that in the case of PPK result from a unique association of mutant Cx26 with Cx43.

RESULTS

PPK mutations are nonfunctional and inhibit wild-type connexins

Cx26-H73R and Cx26-S183F were expressed in *Xenopus* oocytes with other epidermal connexins, and gap junctional conductance, G_j, was measured. Control oocytes injected with water showed negligible conductance ($G_j = 0.12$ μS), whereas cells with wild-type Cx26 channels had an average G_j of 9.3 μS. Cells expressing Cx26-H73R RNA had conductance levels similar to water-injected controls. Cx26-H73R did not display a dominant inhibitory effect on wild-type Cx26, as co-injected cells had a G_j of 9.9 μS (Student's *t*-test $P > 0.05$, compared with Cx26 alone, Figure 1a). Thus, Cx26-H73R failed to form functional gap junction channels when expressed alone.

We then examined interaction with Cx30 and Cx43. Oocyte pairs expressing wild-type Cx30 channels had high conductance ($G_j = 20$ μS, $P < 0.05$). Cell pairs expressing a mixture of Cx26 and Cx30 also produced a mean conductance of 20 μS. Co-expression of wild-type Cx30 and Cx26-H73R resulted in conductance similar to the wild-type controls (Student's *t*-test, $P > 0.05$, Figure 1b), suggesting that Cx26-H73R failed to functionally suppress Cx30 channels. In contrast, Cx26-H73R had a strong inhibitory effect on Cx43. Oocytes expressing Cx43 alone had a mean conductance of 4.6 μS, and cells with both wild-type Cx26 and Cx43 were also well coupled ($G_j = 6.8$ μS). Co-expression of Cx26-H73R and Cx43 yielded significantly lower conductance than cell pairs expressing Cx43 alone ($G_j = 1.1$ μS, $P < 0.05$, Student's *t*-test, Figure 1c), demonstrating a transdominant inhibition of Cx43 by Cx26-H73R.

Unlike Cx26-H73R, Cx26-S183F inhibited Cx26. Conductance ($G_j = 0.03$ μS) measured in oocytes injected with Cx26-S183F alone was the same as control cells, demonstrating loss of functionality. When Cx26-S183F and Cx26 were co-injected, a mean conductance of 3.2 μS resulted, significantly less than Cx26 alone (8.6 μS, Student's

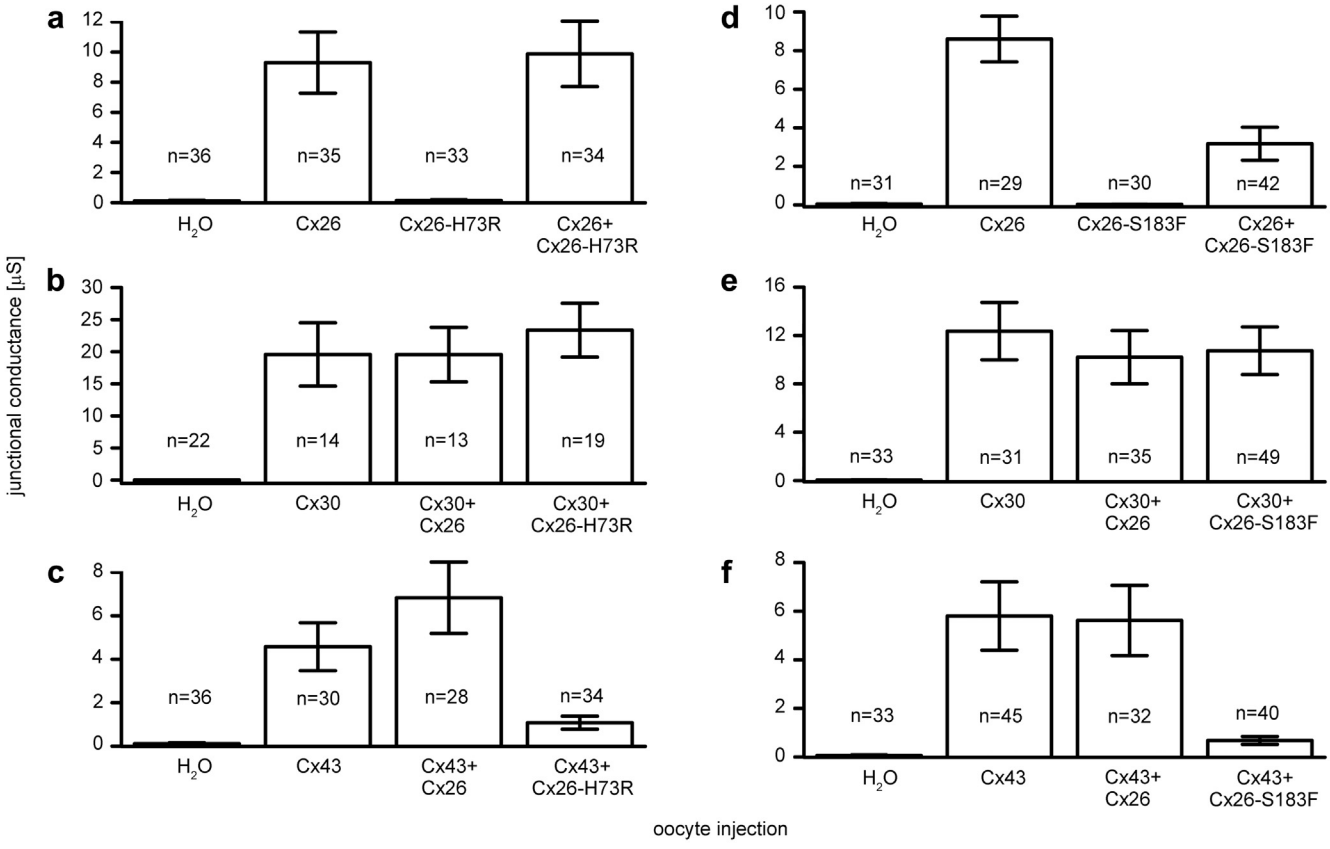

Figure 1. PPK mutations inhibit wild-type Cx43. (**a**) Water-injected cells displayed negligible conductance. Cells expressing Cx26 formed functional channels. Oocytes expressing Cx26-H73R had negligible conductance. Coexpression of Cx26-H73R with Cx26 did not reduce conductance from Cx26 alone. (**b**) Cx30 formed channels when expressed alone or in combination with Cx26-H73R. (**c**) Cx43 formed functional gap junctional channels expressed alone or with Cx26. The combination of Cx43 and Cx26-H73R produced transdominant inhibition of Cx43. (**d**) Oocytes expressing Cx26-S183F had negligible conductance. Coexpression of Cx26-S183F and Cx26 resulted in a significant decrease in conductance ($P < 0.05$) from Cx26 alone. (**e**) Cx30 formed functional channels when expressed alone or in combination with Cx26-S183F. (**f**) Coexpression of Cx43 and Cx26-S183F cRNA resulted in a transdominant inhibition. Data are mean ± standard error.

t-test, $P < 0.05$, Figure 1d). Like Cx26-H73R, Cx26-S183F failed to inhibit Cx30 (Figure 1e). Cx26-S183F also displayed transdominant inhibition of Cx43. Cx26-S183F significantly inhibited Cx43 when both were present in oocytes (G_j = 0.62 μS, $P < 0.05$, Student's *t*-test, Figure 1f). Cx26-S183F displayed a potent inhibition of both wild-type Cx26 and Cx43. Finally, neither mutant was able to form functional heterotypic channels with either wild-type Cx26 (see Supplementary Figure S1, online) or Cx43 (see Supplementary Figure S2, online). These data suggest that Cx26-H73R and Cx26-S183F may result in PPK through an interaction between the mutant and Cx43.

PPK mutants alter Cx43 voltage gating

Physical interaction between Cx43 and Cx26-H73R or Cx26-S183F could modify voltage gating. To examine this, gating of Cx43 channels in the presence and absence of mutant Cx26 was analyzed by subjecting oocyte pairs to hyperpolarizing and depolarizing transjunctional potentials (V_j) while recording junctional currents (I_j). I_js of Cx26 channels displayed asymmetric gating at higher voltages as described previously (Barrio et al., 1991; Bruzzone et al., 2003) (Figure 2a), whereas the I_js of Cx43 channels decreased more symmetrically in a voltage-dependent manner (Bukauskas et al., 2001; Valiunas et al., 2001; White et al., 1994) (Figure 2b). Channels in cell pairs expressing both Cx43 and Cx26-H73R (Figure 2c) or Cx26-S183F (Figure 2d) behaved differently. Despite the inability of the mutants to form functional channels by themselves or heterotypic channels with Cx43, they shifted the behavior of Cx43 to a more asymmetric voltage response, reminiscent of Cx26.

Steady-state gating was quantified by plotting V_j against G_j and fitting a Boltzmann equation. Analysis of the fits of Cx26 and Cx43 showed an asymmetric and symmetric response, respectively (Figure 2e and f). Channels containing Cx43 and Cx26-H73R (Figure 2g) or Cx26-S183F (Figure 2h) displayed gating that resembled Cx43 alone, with additional asymmetric decay at higher potentials. The Boltzmann parameters (Table 1) showed that mixed channels had adopted properties of Cx26, while retaining elements of Cx43 gating. Like Cx43, channels containing both Cx43 and mutant Cx26 had a change in minimum conductance values between negative and positive V_js. The potential for Cx43 at which G_j was halfway to minimum conductance value were similar at positive and negative V_js. In contrast, mixed channels had asymmetric voltage measured midway through the G_j decline. The gain of asymmetry suggests interaction between mutant and wild-type proteins.

Gating kinetics of channels containing Cx43 and mutant Cx26 were also modified. Time constants were determined by plotting current decay and fitting to a monoexponential function. Representative current decays at +120 mV showed Cx43 channels closed slower (Figure 3a) than channels containing both Cx43 and the mutants (Figure 3b and c). Mixed channels containing Cx43 and Cx26-H73R closed 73% faster than Cx43, with mean closure times of 0.24 seconds versus 0.90 seconds. Channels containing Cx43 and Cx26-S183F closed 53% faster, with a mean closure time of 0.42 seconds ($P < 0.05$, one-way analysis of variance [ANOVA], Figure 3d). At potentials of −120 mV, mixed channels had slower channel closure times than wild-type Cx43 (Figure 3e). The acquisition of Cx26-like properties was seen in the kinetics of mixed mutant and Cx43 channels when compared with Cx43 alone. The mutants exhibited a lack of gap junction channel activity when expressed alone, in a homotypic or heterotypic configurations; however, when co-expressed with Cx43 in the same cell, they were able to alter the current decay and shift the equilibrium properties of the channel toward a Cx26-like behavior.

Reduced conductance is not due to lack of mutant protein expression

Syntheses of wild-type and mutant connexins were examined by Western blotting. Immunoblotting for Cx26 revealed ~26-kDa bands in lanes corresponding to oocytes injected with either Cx26 or Cx26-H73R (Figure 4a, arrowhead). A nonspecific band was also detected in all lanes by the Cx26 antibody used (asterisk). The Cx43 antibody showed ~43-kDa bands in oocytes injected with Cx43 cRNA, whether alone or in combination with Cx26 or Cx26-H73R (Figure 4b). When the Cx43 blot was reprobed for β-actin, it was detected at similar intensity in all samples, confirming equal protein loading (Figure 4c). Band densitometry on replicate blots ($n = 4$) revealed no significant differences between the expression of Cx26 alone, Cx26-H73R alone, and the wild-type and mutant in combination with wild-type Cx43 ($P < 0.05$, Figure 4d). The plot for the normalized intensity of Cx43 protein also failed to show significant differences between the samples ($P < 0.05$, one-way ANOVA, Figure 4e).

In contrast, Cx26-S183F showed reduced expression compared with Cx26 (Figure 4f). Immunoblotting for Cx43 revealed equivalent protein levels (Figure 4g), thereby attributing the loss of functional activity in the presence of Cx26-S183F to a mechanism not related to the translational efficiency of Cx43. The blot was reprobed for β-actin to ensure equal loading of samples (Figure 4h). Quantification showed that Cx26-S183F was reduced by ~75% compared with Cx26 ($P < 0.05$, one-way ANOVA, Figure 4i). The reduction in mutant protein indicated either reduced translational efficiency or protein stability. Examination of Cx43 band intensity showed equivalent expression in all corresponding lanes (Figure 4j). Although Cx26-S183F expression was lower than Cx26 or Cx26-H73R, the potency with which the mutant was able to affect Cx43 remained high.

Cx26 PPK mutants associate with Cx43

PPK mutants affected the behavior of Cx43, suggesting the possible formation of heteromeric channels. To investigate this, co-immunoprecipitation was performed on cells coexpressing Cx43 and mutant Cx26. Cell lysates showed Cx26 protein present in all lanes containing wild-type or mutant (Figure 5a and e). Reprobing for Cx43 revealed similar expression of protein in lanes containing Cx43 alone or coexpressed with wild-type or mutant Cx26 (Figure 5b and f). Immunoblotting the immunoprecipitate revealed Cx26 protein in samples injected with either wild-type or mutant (Figure 5c and g). As described above, Cx26-S183F expression was lower than wild-type Cx26 or Cx26-H73R. Immunoprecipitates were reprobed to determine if the Cx26 mutants interacted with Cx43. As previously described

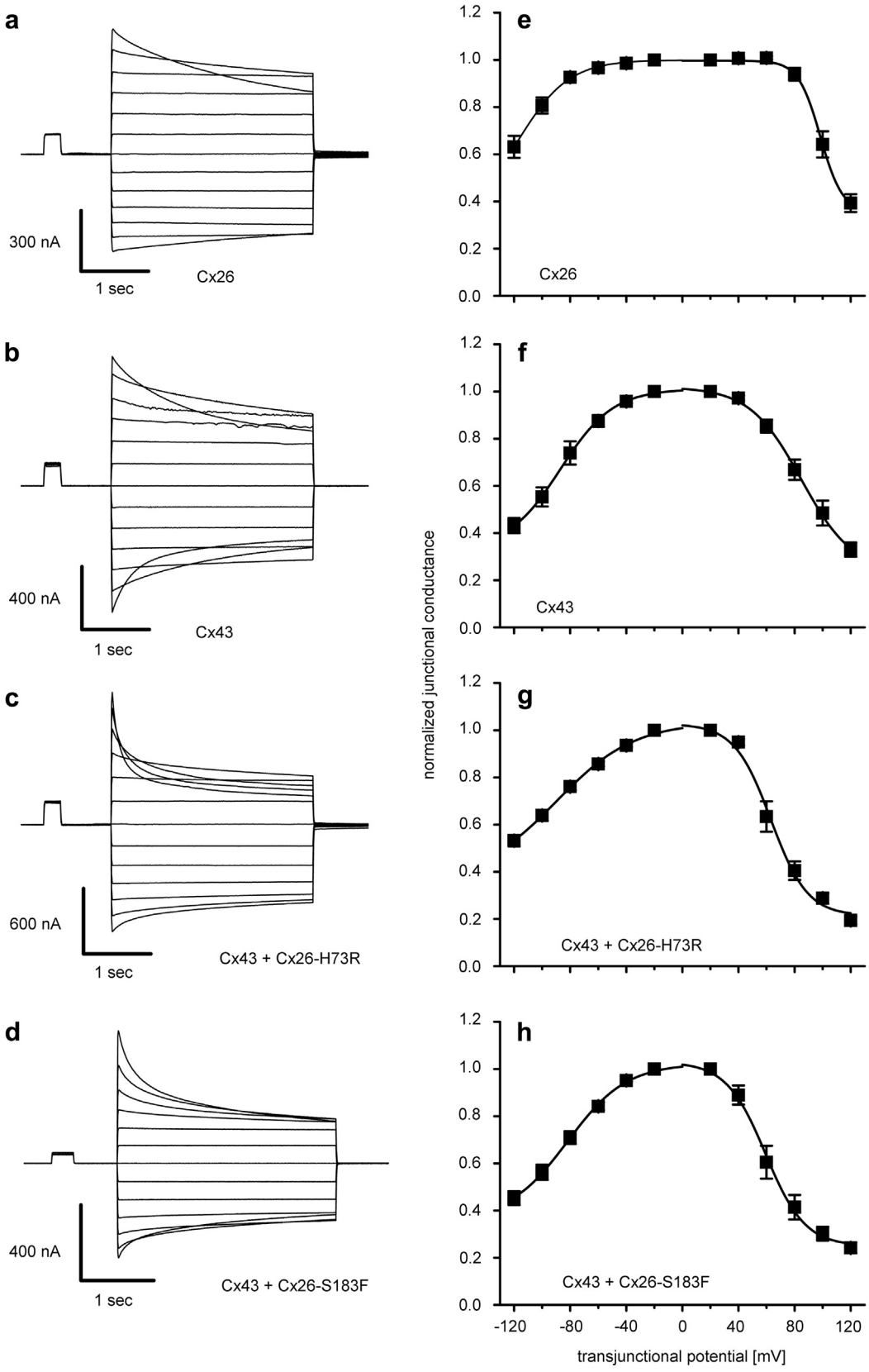

Figure 2. PPK mutants alter voltage gating of Cx43. Recordings of junctional currents in response to transjunctional potentials of opposite polarity revealed that Cx26 (**a**) showed an asymmetry in current decay at higher voltages, whereas Cx43 (**b**) showed a more symmetric decrease in currents in a voltage-dependent manner. In the presence of Cx26-H73R (**c**) or Cx26-S183F (**d**), gating of Cx43 was modified toward a more asymmetric response to voltage. Quantification of gating by fitting steady-state conductance to a Boltzmann equation revealed pronounced asymmetry for Cx26 (**e**) at negative and positive potentials ($n = 7$). Cx43 (**f**) showed a more symmetric decay ($n = 6$). Mixed channels containing Cx26-H73R (**g**, $n = 4$) or Cx26-S183F (**h**, $n = 7$) shifted Cx43 gating properties toward an asymmetric behavior, reminiscent of Cx26.

Table 1. Boltzmann parameters of gap junction channels

Oocyte injection	V_j	G_{min}	V_0 (mV)	A
Cx26	+	0.35 ± 0.01	98 ± 0.4	0.13
Cx26	−	0.31 ± 0.14	−118 ± 7.2	0.05
Cx43	+	0.24 ± 0.05	85 ± 2.7	0.05
Cx43	−	0.33 ± 0.03	−87 ± 1.8	0.05
Cx26-H73R+Cx43	+	0.21 ± 0.04	63 ± 3.1	0.08
Cx26-H73R+Cx43	−	0.36 ± 0.09	−90 ± 7.4	0.04
Cx26-S183F+Cx43	+	0.25 ± 0.03	59 ± 2.3	0.07
Cx26-S183F+Cx43	−	0.36 ± 0.04	−82 ± 2.8	0.05

+ and −, transjunctional membrane potential polarity; A, cooperativity constant, reflecting the number of charges moving through the transjunctional field; G_{min}, minimum conductance value; V_0, voltage measured midway through the G_j decline.

(Gemel et al., 2004; Yum et al., 2010), Cx26 inefficiently co-immunoprecipitated Cx43. Levels of Cx43 protein in the samples coexpressing Cx43 and either Cx26 mutant were much higher, suggesting the mutant proteins were able to more efficiently co-immunoprecipitate with Cx43 (Figure 5d and h). These findings show association of mutant Cx26 and Cx43 in heteromeric connexins, providing a potential mechanism whereby mutant Cx26 was able to modify Cx43 activity.

Cx26 PPK mutants do not form functional hemichannels

KID syndrome mutations routinely form active hemichannels (Gerido et al., 2007; Mhaske et al., 2013; Sanchez et al., 2010; Stong et al., 2006); however, it is not known if PPK mutations behave similarly. Thus, hemichannel activity was analyzed by expression of Cx26, Cx26-H73R, and Cx26-S183F in single oocytes. Water-injected control oocytes showed limited current flow at all voltage steps (Figure 6a).

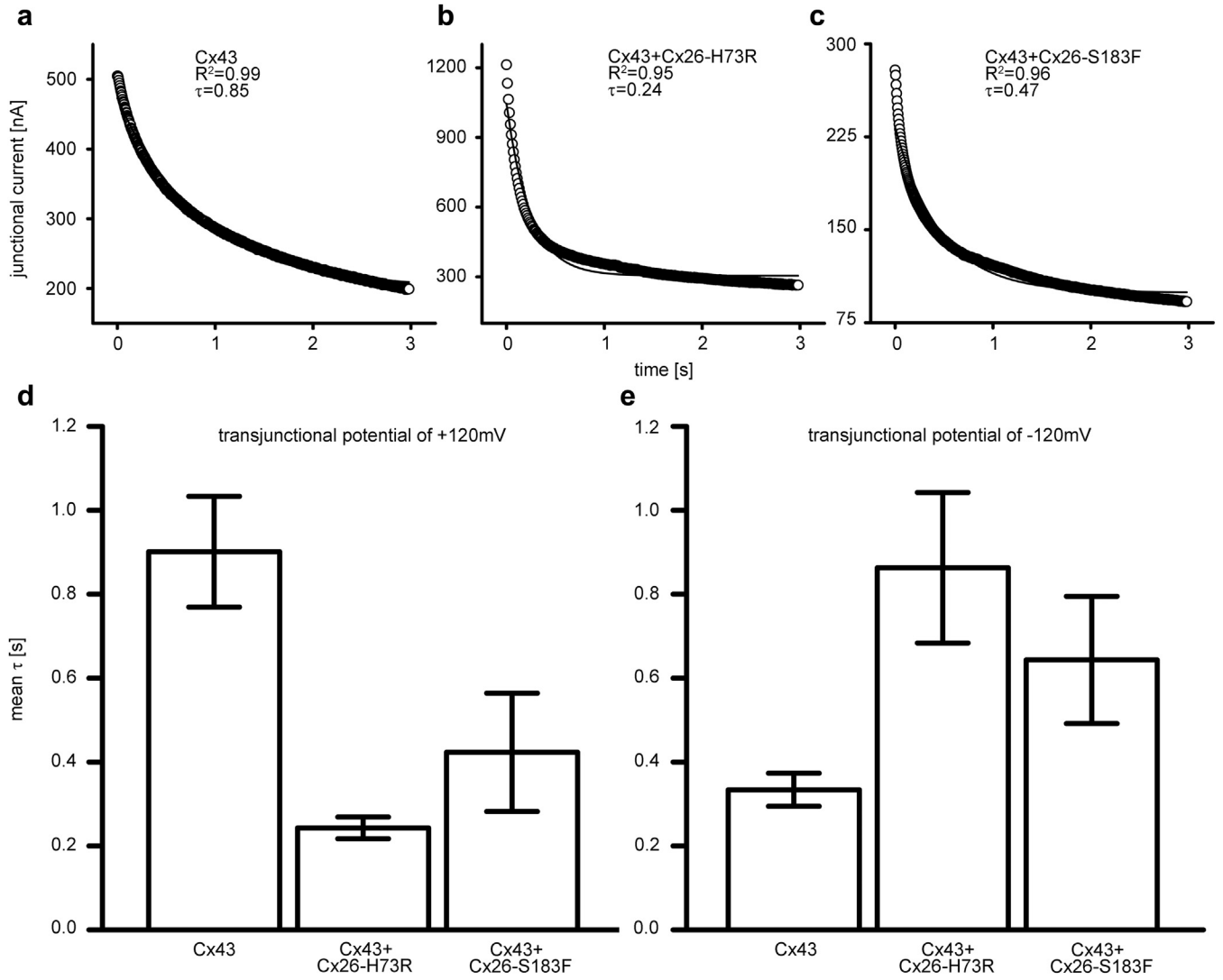

Figure 3. PPK mutants modify Cx43 channel closure kinetics. Junctional currents were fit to a single exponential decay to determine tau (τ). Representative decays at V_j = +120 mV showed slower closure kinetics in Cx43 channels (**a**), whereas the presence of mutant Cx26-H73R (**b**) or Cx26-S183F (**c**) resulted in decreased τ values. (**d**) At +120 mV, mean τ values were 0.90 ± 0.26 for Cx43 alone ($n = 4$), 0.24 ± 0.05 for Cx43+Cx26-H73R ($n = 4$), and 0.42 ± 0.31 ($n = 5$) for Cx43+Cx26-S183F. (**e**) At −120 mV, where Cx43 alone closed faster than it did in the presence of mutant Cx26. Mean τ values were 0.33 ± 0.07 for Cx43 alone ($n = 4$), 0.86 ± 0.36 for Cx43+Cx26-H73R ($n = 4$), and 0.64 ± 0.34 ($n = 5$) for Cx43+Cx26-S183F. Data are mean ± standard error.

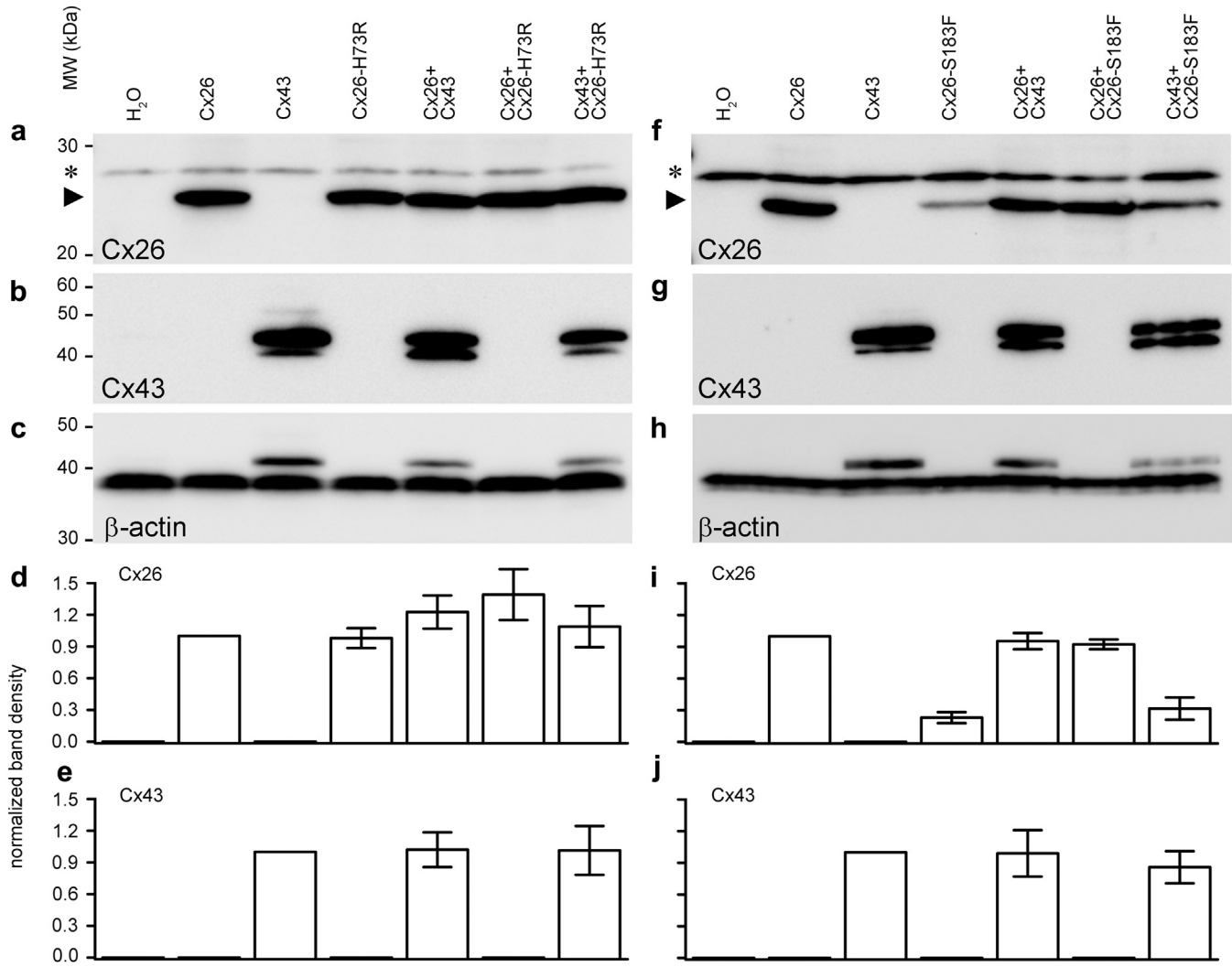

Figure 4. Expression of connexin proteins in *Xenopus* oocytes. (**a**) Immunoblot analysis of oocytes expressing Cx26 and Cx26-H73R showed equal expression of protein in all lanes. (**b, g**) Cx43 levels were the same in each condition. (**c, h**) Reprobing the Cx43 blots for β-actin confirmed equal loading. (**f**) Analysis of oocytes expressing Cx26 and Cx26-S183F revealed qualitatively lower expression of the mutant protein as compared with wild-type. (**d**) Band densitometry ($n = 4$) quantitatively confirmed that mean Cx26 and Cx26-H73R protein expression was equivalent in all conditions tested. (**e, j**) Cx43 levels ($n = 4$) were also equal across experiments. (**i**) Cx26-S183F protein expression showed an ~75% reduction compared with Cx26 ($n = 4$). Data are mean ± standard error.

As previously characterized (Gerido et al., 2007; Gonzalez et al., 2006; Lee et al., 2009; Mhaske et al., 2013; Ripps et al., 2004; Sanchez et al., 2010, 2013), Cx26 hemichannel activity resulted in outward currents upon depolarization (Figure 6b). Cx26-H73R and Cx26-S183F showed greatly reduced membrane current compared with Cx26 injected cells (Figure 6c and d). Mean membrane currents were plotted against membrane voltage to quantify differences in activity. Cx26 expressing cells showed large outward currents that increased with greater depolarization (Figure 6e). At +60 mV, Cx26 produced currents that were an order of magnitude larger than controls, as well as both Cx26-H73R and Cx26-S183F mutants ($P < 0.05$). The mutant injected cells were indistinguishable from water-injected negative control cells, suggesting loss of native hemichannel activity. Coexpression of Cx26-H73R and Cx26-S183F with wild-type Cx26 produced a reduction in hemichannel activity (see Supplementary Figure S3, online).

Cx26 PPK mutants enhance Cx43 hemichannels

Cx26 PPK mutants altered the activity of Cx43 gap junctions through an association of Cx43 with mutant Cx26 in heteromeric hemichannels. Thus, we examined if Cx26 mutants associated with PPK could also alter Cx43 hemichannel activity. Oocytes expressing Cx43 exhibited no hemichannel activity (Figure 6f), as previously reported (White et al., 1999). Although Cx43, Cx26-H73R, and Cx26-S183F were all unable to form hemichannels alone, heteromeric hemichannels composed of Cx43 with either Cx26-H73R, or Cx26-S183F, showed significantly higher current flow (Figure 6g and h). Quantification of the data indicated a marked increase in hemichannel activity in cells coexpressing Cx26-H73R and Cx43 at increasing voltages, demonstrating acquired hemichannel function (Figure 6i). We observed a similar, albeit less consistent, trend in cells coexpressing Cx26-S183F and Cx43. Of 55 oocytes recorded, 33% ($n = 18$) showed a clear difference in hemichannel

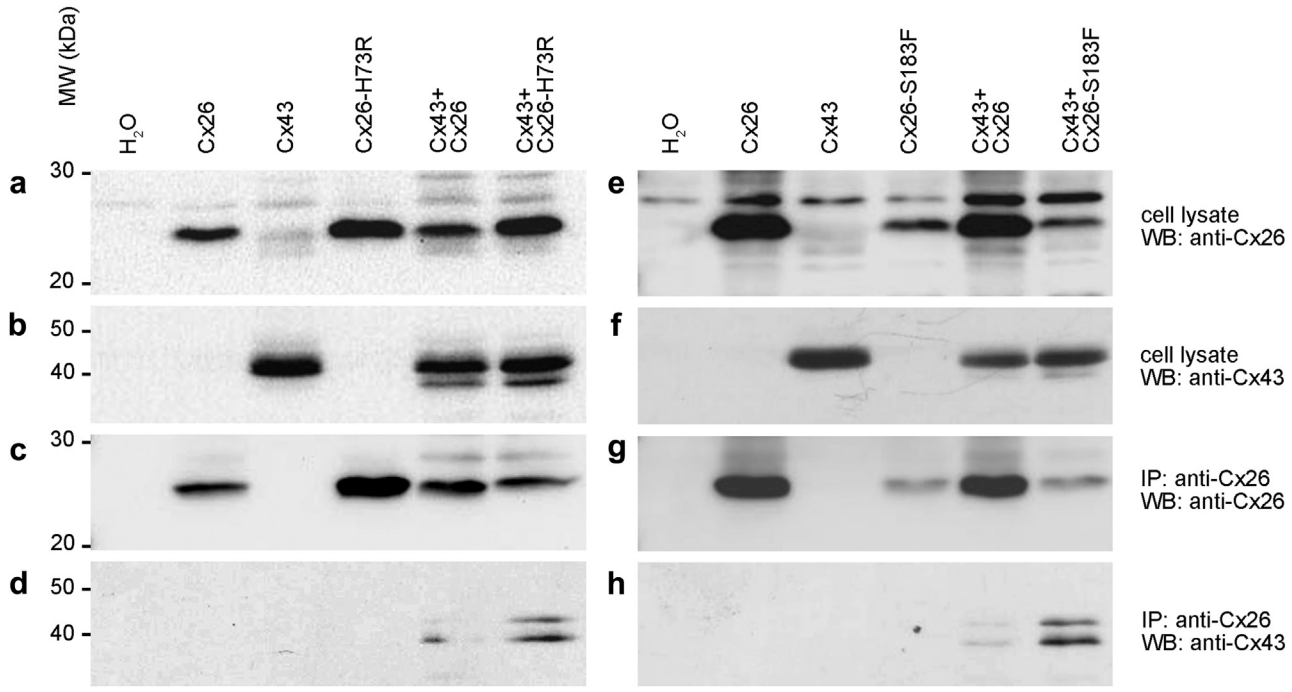

Figure 5. PPK mutants biochemically interact with Cx43. (**a, e**) Western blot (WB) analysis of cell lysates showed qualitatively similar expression of Cx26 and Cx26-H73R and reduced protein expression of Cx26-S183F. (**b, f**) Detection of Cx43 in the cell lysates revealed equal protein expression in corresponding lanes. (**c, g**) Immunoprecipitation (IP) of Cx26 and subsequent detection of Cx26 protein showed the presence of the protein in all samples containing either wild-type or mutant. (**d, h**) Co-immunoprecipitation and WB analysis of Cx43 revealed enhanced formation of heteromeric channels containing Cx43 and mutant Cx26.

activity from Cx43 expressing cells, whereas the remaining cells failed to produce membrane currents greater than controls. Differences between hemichannel currents produced by Cx43 alone and Cx43 coexpressed with Cx26-H73R or Cx26-S183F were statistically significant ($P < 0.05$, one-way ANOVA). Thus, Cx43 and the mutants Cx26-H73R and Cx26-S183F were able to form functional hemichannels when coexpressed as heteromeric connexons.

DISCUSSION

We studied two Cx26 mutations associated with PPK and deafness. Cx26-H73R and Cx26-S183F were unable to form functional homomeric hemichannels or gap junctions when expressed alone. However, upon introduction to cells expressing Cx43, they reduced Cx43 gap junctional activity, altered channel gating, and increased hemichannel activity. Co-immunoprecipitation of Cx43 and mutant Cx26 showed the formation of heteromeric connexons. This acquired gain of function distinguishes Cx26 mutations associated with PPK from other Cx26 syndromic disorders such as KID syndrome. The ability of both mutants to modify Cx43 hemichannels and gap junctions brings into focus an emerging role of Cx43 in the causation of epidermal disorders and highlights common attributes of Cx26 mutations linked to PPK.

We previously analyzed the functional properties of three Cx26 mutants causing PPK and deafness, Cx26-R75W, Cx26-δE42, and Cx26-D66H. All the mutants lacked intrinsic gap junction channel activity and inhibited coexpressed wild-type Cx26 (Richard et al., 1998; Rouan et al., 2001). When coexpressed with Cx43, the mutants all produced a strong inhibition of Cx43 coupling (Rouan et al., 2001). This model of transdominant inhibition of Cx43 was supported by study of the Cx26-G59A mutation associated with PPK and deafness showing that Cx26-G59A failed to form channels by itself and also inhibited intercellular dye transfer when coexpressed with Cx43 (Thomas et al., 2004). Thus, transdominant interactions between Cx26 mutations and Cx43 could reduce overall coupling between epidermal keratinocytes, contributing to skin diseases like PPK.

Accumulating data suggest that syndromic Cx26 mutations causing skin disease acquire new functional activities. To date, all tested PPK mutations were devoid of any intrinsic homomeric channel activity. In contrast, KID mutations form constitutively active homomeric hemichannels, and many can form functional homomeric gap junction channels (Gerido et al., 2007; Lee et al., 2009; Sanchez et al., 2010). Thus, two mechanisms have emerged for skin disease linked Cx26 mutations: (i) inhibition of other keratinocyte connexins and (ii) formation of aberrant hemichannels. Transdominant inhibition would decrease the number of connexin types contributing to intercellular communication in the epidermis. Active hemichannels would produce extracellular release of metabolites, potentially adversely influencing neighboring cells or initiating apoptosis. Additional characterization of disease causing mutations will further our understanding of the pathophysiology of skin diseases where connexin activity has been compromised.

Cx43 is expressed across the epidermis (Butterweck et al., 1994; Kamibayashi et al., 1993), and mutant Cx26 expression is upregulated in patients with PPK and colocalizes with Cx43 (Rouan et al., 2001). Mutations in *GJA1*, encoding Cx43, result in oculodentodigital dysplasia

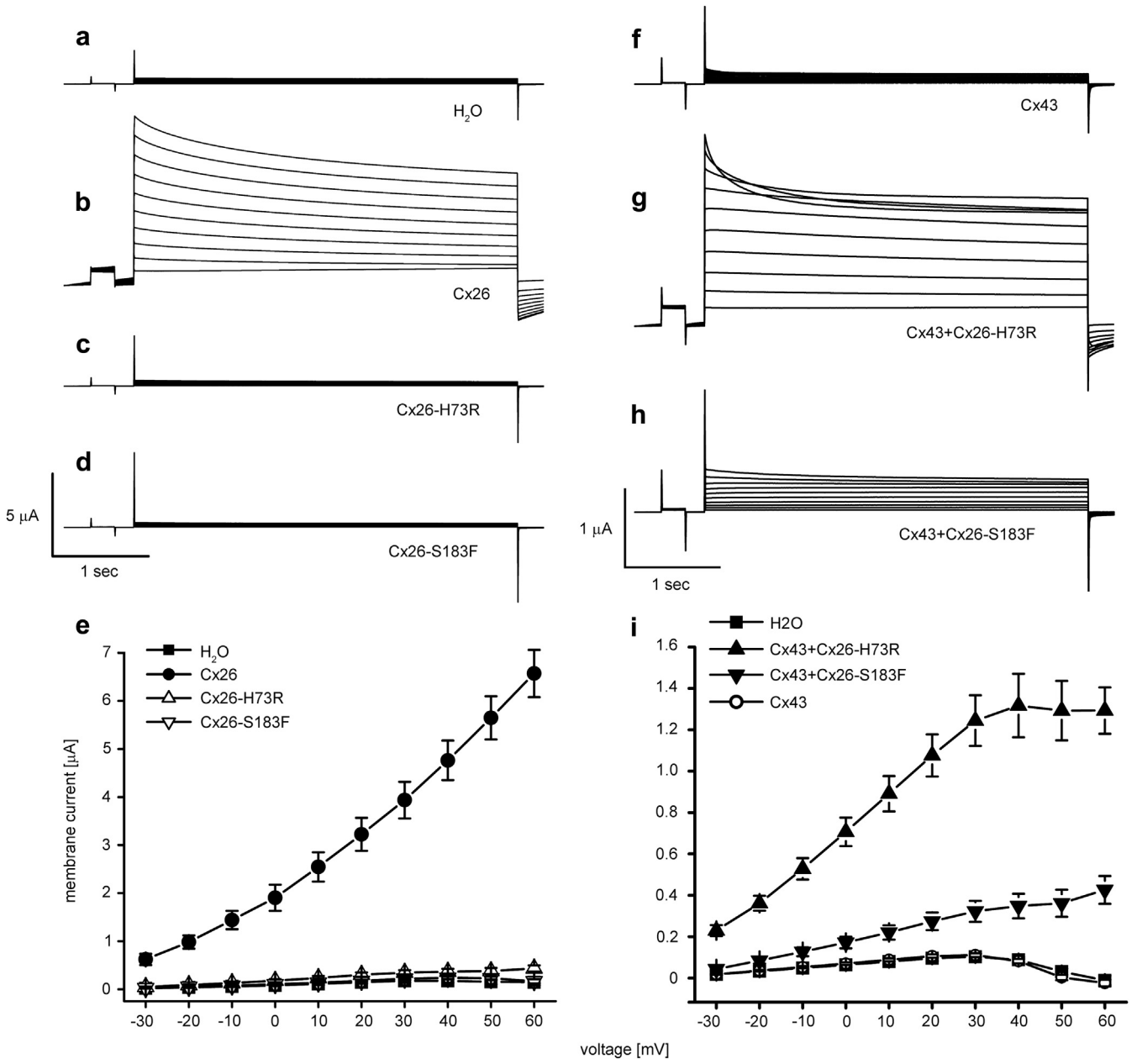

Figure 6. PPK mutants lack hemichannel activity but stimulate Cx43 hemichannels when coexpressed. (**a**) Oocytes injected with water exhibited minimal currents. (**b**) Cx26 cells displayed current that increased at each voltage step. Cx26-H73R (**c**) and Cx26-S183F (**d**) lacked hemichannel currents. (**e**) Steady-state currents for water-injected cells were negligible at all voltages ($n = 12$). Cx26 currents increased with depolarization ($n = 8$). Cx26-H73R ($n = 9$) and Cx26-S183F ($n = 9$) currents were negligible. (**f**) Cx43 cells lacked hemichannel activity. When coexpressed with Cx26-H73R (**g**) or Cx26-S183F (**h**), Cx43 showed increased hemichannel activity. (**i**) Steady-state currents for H_2O ($n = 21$) or Cx43 ($n = 21$) cells were negligible. Coexpressing Cx43 and Cx26-H73R ($n = 10$) or Cx26-S183F ($n = 18/55$) enhanced Cx43 hemichannel activity. Data are mean ± standard error.

(Paznekas et al., 2003), erythrokeratodermia variabilis et progressiva (Boyden et al., 2015), and keratoderma-hypotrichosis-leukonychia totalis syndrome (KHLS) (Wang et al., 2015). These disorders share some clinical features with syndromic Cx26 diseases. Oculodentodigital dysplasia manifests with neuropathies, facial and digit abnormalities, and occasionally skin disease (Kogame et al., 2014). Erythrokeratodermia variabilis et progressiva results in hyperkeratosis and transient figurate patches of erythema. KHLS encompasses severe hyperkeratosis, congenital alopecia, and leukonychia.

There are similarities between clinical features observed in patients with Cx26 and Cx43 mutations. The presence of hyperkeratotic lesions on frictional surfaces (palms and soles) points to possible mechanistic similarities through which PPK arises. Additionally, KHLS shares clinical correlations with Bart-Pumphrey syndrome, caused by Cx26 mutations, including hyperkeratosis and leukonychia (Bart and Pumphrey, 1967). Despite phenotypic similarities, functional studies of Cx43 mutations need to be completed to establish definitive mechanistic correlations. Expression of the Cx43-G8V mutation resulting in KHLS resulted in the

formation of hemichannels, allowing an influx of Ca^{2+} into cells (Wang et al., 2015). Aberrant hemichannel formation was frequently observed in KID syndrome and in heteromeric connexons containing Cx43 and Cx26 PPK mutants (Figure 6). Another recent study demonstrated increased Cx43 hemichannel activity in the presence of the only non-hemichannel forming KID mutation, Cx26-S17F (Garcia et al., 2015). Consistent with our data, Cx26-S17F was unable to form hemichannels or gap junctions alone but increased Cx43 hemichannel activity when coexpressed. These findings highlight a growing importance of Cx43 in epidermal disorders, resulting not only from mutations in *GJA1* but also from the *GJB2* gene.

MATERIALS AND METHODS

In vitro transcription, oocyte microinjection, and pairing

Cx26, Cx30, and Cx43 were cloned into pCS2+ expression vector for functional studies in *Xenopus* oocytes (DeRosa et al., 2009; Turner and Weintraub, 1994). Cx26-H73R and Cx26-S183F constructs were prepared by site directed mutagenesis (Horton et al., 1990). DNA constructs were cloned into pBlueScript II (Agilent Technologies, Santa Clara, CA) and sequenced before subcloning into pCS2+. Constructs were linearized and transcribed using SP6 mMessage mMachine (Ambion, Austin, TX). Oocytes were collected from *Xenopus laevis* females and cultured in modified Barth's medium (Mhaske et al., 2013). Oocytes were injected with 10 ng of antisense *Xenopus* Cx38 oligonucleotide (Barrio et al., 1991; Bruzzone et al., 1993), followed by connexin transcripts (5 ng/cell) alone or in combination. Water-injected oocytes served as a negative control. Cx43 RNA was injected at a concentration that would yield average electrical conductance of ~5–10 μS. Other cRNA was injected at comparable levels.

Recording of hemichannel currents

Hemichannel currents were recorded 24 hours after cRNA injection using a GeneClamp 500 amplifier controlled by a PC-compatible computer through a Digidata 1440A interface using pClamp 8.0 software (Axon Instruments, Foster City, CA). Electrodes (1.5-mm diameter glass; World Precision Instruments, Sarasota, FL) were pulled to a resistance of 1–2 MΩ (Narishige, Tokyo, Japan) and filled with 3 M KCl, 10 mM EGTA, and 10 mM HEPES, pH 7.4. Oocytes were recorded in modified Barth's medium without added calcium (Gerido et al., 2007). Hemichannel current-voltage curves were obtained by clamping cells at −40 mV and subjecting them to 5-second depolarizing voltage steps ranging from −30 to +60 mV in 10-mV increments.

Recording of junctional conductance

G_j was measured by initially clamping both cells in a pair at −40 mV (a V_j of zero). One cell was subjected to alternating pulses of ±20 mV, and the current produced by the change in voltage was recorded in the second cell, which was equal in magnitude to the I_j. Conductance was calculated by dividing I_j by the voltage difference, $G_j = I_j/(V1 - V2)$ (Spray et al., 1981). Gating properties were determined by recording the junctional current in response to hyperpolarizing or depolarizing V_js in 20-mV steps. Steady-state currents (I_{jss}) were measured at the end of the voltage pulse. Steady-state conductance (G_{jss}) was calculated by dividing I_{jss} by V_j, normalized to ±20 mV, and plotted against V_j. Data were fit to a Boltzmann relation: $G_{jss} = (G_{jmax} - G_{jmin})/(1+ \exp [A (V_j - V_0)]) + G_{jmin}$, where G_{jmax} is the maximum conductance, G_{jmin} is the residual conductance, and V_0 is the transjunctional voltage at which $G_{jss} = (G_{jmax} - G_{jmin})/2$. A ($=nq/kT$) represents the number (n) of electron charges (q) moving through the membrane, where k is the Boltzmann constant and T is the absolute temperature.

Western blotting

Oocytes extracts were prepared as previously described (White et al., 1992), separated on 12% SDS gels and transferred to nitrocellulose membranes. Blots were blocked with 5% milk 0.1% Tween 20 in Tris-buffered saline, probed with polyclonal antibodies against Cx26 or Cx43 (Life Technologies, Carlsbad, CA), followed by horseradish peroxidase conjugated secondary antibodies (Jackson ImmunoResearch, West Grove, PA, and GE Healthcare, Piscataway, NJ). A monoclonal β-actin antibody (Abcam, Cambridge, MA) was used as a loading control. Band intensities were quantified using ImageJ software (National Institutes of Health, Bethesda, MD). The phosphorylated and nonphosphorylated forms of Cx43 (two bands) were quantified and expressed as a single value.

Co-Immunoprecipitation

For cell lysate analysis, the membrane fraction was resuspended in SDS sample buffer. For co-immunoprecipitation, the membrane fraction was resuspended in radioimmunoprecipitation assay buffer (Yum et al., 2007). Samples were precleared with protein G agarose beads (Roche, Mannheim, Germany) that had been blocked overnight in 5% BSA-phosphate-buffered saline and incubated with a monoclonal Cx26 antibody (Life Technologies). Protein G agarose beads were added to the samples and incubated. Beads were then washed, boiled in SDS sample buffer, and eluted proteins were run on gels. Proteins were detected using polyclonal antibodies against Cx26 or Cx43.

CONFLICT OF INTEREST

The authors state no conflict of interest.

ACKNOWLEDGMENTS

This work was supported by National Institutes of Health grant R01 AR59505 (to TWW) from the National Institute of Arthritis and Musculoskeletal and Skin Diseases.

SUPPLEMENTARY MATERIAL

Supplementary material is linked to the online version of the paper at www.jidonline.org, and at http://dx.doi.org/10.1038/JID.2015.389.

REFERENCES

Bakirtzis G, Choudhry R, Aasen T, et al. Targeted epidermal expression of mutant Connexin 26(D66H) mimics true Vohwinkel syndrome and provides a model for the pathogenesis of dominant connexin disorders. Hum Mol Genet 2003;12:1737–44.

Barrio LC, Suchyna T, Bargiello T, et al. Gap junctions formed by connexins 26 and 32 alone and in combination are differently affected by applied voltage. Proc Natl Acad Sci USA 1991;88:8410–4.

Bart RS, Pumphrey RE. Knuckle pads, leukonychia and deafness. A dominantly inherited syndrome. N Engl J Med 1967;276:202–7.

Bevans CG, Kordel M, Rhee SK, et al. Isoform composition of connexin channels determines selectivity among second messengers and uncharged molecules. J Biol Chem 1998;273:2808–16.

Blanpain C, Fuchs E. Epidermal stem cells of the skin. Annu Rev Cell Dev Biol 2006;22:339–73.

Blanpain C, Fuchs E. Epidermal homeostasis: a balancing act of stem cells in the skin. Nat Rev Mol Cell Biol 2009;10:207–17.

Boyden LM, Craiglow BG, Zhou J, et al. Dominant de novo mutations in GJA1 cause erythrokeratodermia variabilis et progressiva, without features of oculodentodigital dysplasia. J Invest Dermatol 2015;135:1540–7.

Brissette JL, Kumar NM, Gilula NB, et al. Switch in gap junction protein expression is associated with selective changes in junctional permeability during keratinocyte differentiation. Proc Natl Acad Sci USA 1994;91:6453–7.

Bruzzone R, Haefliger JA, Gimlich RL, et al. Connexin40, a component of gap junctions in vascular endothelium, is restricted in its ability to interact with other connexins. Mol Biol Cell 1993;4:7–20.

Bruzzone R, Veronesi V, Gomes D, et al. Loss-of-function and residual channel activity of connexin26 mutations associated with non-syndromic deafness. FEBS Lett 2003;533:79–88.

Bukauskas FF, Bukauskiene A, Bennett MV, et al. Gating properties of gap junction channels assembled from connexin43 and connexin43 fused with green fluorescent protein. Biophys J 2001;81:137–52.

Butterweck A, Elfgang C, Willecke K, et al. Differential expression of the gap junction proteins connexin45, -43, -40, -31, and -26 in mouse skin. Eur J Cell Biol 1994;65:152–63.

Caputo R, Peluchetti D. The junctions of normal human epidermis. A freeze-fracture study. J Ultrastruct Res 1977;61:44–61.

de Zwart-Storm EA, Hamm H, Stoevesandt J, et al. A novel missense mutation in GJB2 disturbs gap junction protein transport and causes focal palmoplantar keratoderma with deafness. J Med Genet 2008a;45:161–6.

de Zwart-Storm EA, Rosa RF, Martin PE, et al. Molecular analysis of connexin26 asparagine14 mutations associated with syndromic skin phenotypes. Exp Dermatol 2011a;20:408–12.

de Zwart-Storm EA, van Geel M, van Neer PA, et al. A novel missense mutation in the second extracellular domain of GJB2, p.Ser183Phe, causes a syndrome of focal palmoplantar keratoderma with deafness. Am J Pathol 2008b;173:1113–9.

de Zwart-Storm EA, van Geel M, Veysey E, et al. A novel missense mutation in GJB2, p.Tyr65His, causes severe Vohwinkel syndrome. Br J Dermatol 2011b;164:197–9.

DeRosa AM, Mese G, Li L, et al. The cataract causing Cx50-S50P mutant inhibits Cx43 and intercellular communication in the lens epithelium. Exp Cell Res 2009;315:1063–75.

Di WL, Rugg EL, Leigh IM, et al. Multiple epidermal connexins are expressed in different keratinocyte subpopulations including connexin 31. J Invest Dermatol 2001;117:958–64.

Garcia IE, Maripillan J, Jara O, et al. Keratitis-ichthyosis-deafness syndrome-associated cx26 mutants produce nonfunctional gap junctions but hyperactive hemichannels when co-expressed with wild type cx43. J Invest Dermatol 2015;135:1338–47.

Gemel J, Valiunas V, Brink PR, et al. Connexin43 and connexin26 form gap junctions, but not heteromeric channels in co-expressing cells. J Cell Sci 2004;117:2469–80.

Gerido DA, DeRosa AM, Richard G, et al. Aberrant hemichannel properties of Cx26 mutations causing skin disease and deafness. Am J Physiol Cell Physiol 2007;293:C337–45.

Goliger JA, Bruzzone R, White TW, et al. Dominant inhibition of intercellular communication by two chimeric connexins. Clin Exp Pharmacol Physiol 1996;23:1062–7.

Gonzalez D, Gomez-Hernandez JM, Barrio LC. Species specificity of mammalian connexin-26 to form open voltage-gated hemichannels. FASEB J 2006;20:2329–38.

Goodenough DA, Paul DL. Beyond the gap: functions of unpaired connexon channels. Nat Rev Mol Cell Biol 2003;4:285–94.

Griffith AJ, Yang Y, Pryor SP, et al. Cochleosaccular dysplasia associated with a connexin 26 mutation in keratitis-ichthyosis-deafness syndrome. Laryngoscope 2006;116:1404–8.

Guo H, Acevedo P, Parsa FD, et al. Gap-junctional protein connexin 43 is expressed in dermis and epidermis of human skin: differential modulation by retinoids. J Invest Dermatol 1992;99:460–7.

Horton RM, Cai ZL, Ho SN, et al. Gene splicing by overlap extension: tailor-made genes using the polymerase chain reaction. Biotechniques 1990;8:528–35.

Janecke AR, Hennies HC, Gunther B, et al. GJB2 mutations in keratitis-ichthyosis-deafness syndrome including its fatal form. Am J Med Genet A 2005;133A:128–31.

Jonard L, Feldmann D, Parsy C, et al. A familial case of keratitis-ichthyosis-deafness (KID) syndrome with the GJB2 mutation G45E. Eur J Med Genet 2008;51:35–43.

Kam E, Melville L, Pitts JD. Patterns of junctional communication in skin. J Invest Dermatol 1986;87:748–53.

Kamibayashi Y, Oyamada M, Oyamada Y, et al. Expression of gap junction proteins connexin 26 and 43 is modulated during differentiation of keratinocytes in newborn mouse epidermis. J Invest Dermatol 1993;101:773–8.

Kanno Y, Loewenstein WR. Low-resistance coupling between gland cells. some observations on intercellular contact membranes and intercellular space. Nature 1964;201:194–5.

Kogame T, Dainichi T, Shimomura Y, et al. Palmoplantar keratosis in oculodentodigital dysplasia with a GJA1 point mutation out of the C-terminal region of connexin 43. J Dermatol 2014;41:1095–7.

Lawrence TS, Beers WH, Gilula NB. Transmission of hormonal stimulation by cell-to-cell communication. Nature 1978;272:501–6.

Lee JR, Derosa AM, White TW. Connexin mutations causing skin disease and deafness increase hemichannel activity and cell death when expressed in *Xenopus* oocytes. J Invest Dermatol 2009;129:870–8.

Lee JR, White TW. Connexin-26 mutations in deafness and skin disease. Expert Rev Mol Med 2009;11:e35.

Maestrini E, Korge BP, Ocana-Sierra J, et al. A missense mutation in connexin26, D66H, causes mutilating keratoderma with sensorineural deafness (Vohwinkel's syndrome) in three unrelated families. Hum Mol Genet 1999;8:1237–43.

Mazereeuw-Hautier J, Bitoun E, Chevrant-Breton J, et al. Keratitis-ichthyosis-deafness syndrome: disease expression and spectrum of connexin 26 (GJB2) mutations in 14 patients. Br J Dermatol 2007;156:1015–9.

Mhaske PV, Levit NA, Li L, et al. The human Cx26-D50A and Cx26-A88V mutations causing keratitis-ichthyosis-deafness syndrome display increased hemichannel activity. Am J Physiol Cell Physiol 2013;304:C1150–8.

Paznekas WA, Boyadjiev SA, Shapiro RE, et al. Connexin 43 (GJA1) mutations cause the pleiotropic phenotype of oculodentodigital dysplasia. Am J Hum Genet 2003;72:408–18.

Richard G, Brown N, Ishida-Yamamoto A, et al. Expanding the phenotypic spectrum of Cx26 disorders: Bart-Pumphrey syndrome is caused by a novel missense mutation in GJB2. J Invest Dermatol 2004;123:856–63.

Richard G, White TW, Smith LE, et al. Functional defects of Cx26 resulting from a heterozygous missense mutation in a family with dominant deafmutism and palmoplantar keratoderma. Hum Genet 1998;103:393–9.

Ripps H, Qian H, Zakevicius J. Properties of connexin26 hemichannels expressed in *Xenopus* oocytes. Cell Mol Neurobiol 2004;24:647–65.

Risek B, Klier FG, Gilula NB. Multiple gap junction genes are utilized during rat skin and hair development. Development 1992;116:639–51.

Rouan F, White TW, Brown N, et al. Trans-dominant inhibition of connexin–43 by mutant connexin–26: implications for dominant connexin disorders affecting epidermal differentiation. J Cell Sci 2001;114:2105–13.

Salomon D, Masgrau E, Vischer S, et al. Topography of mammalian connexins in human skin. J Invest Dermatol 1994;103:240–7.

Sanchez HA, Mese G, Srinivas M, et al. Differentially altered Ca2+ regulation and Ca2+ permeability in Cx26 hemichannels formed by the A40V and G45E mutations that cause keratitis ichthyosis deafness syndrome. J Gen Physiol 2010;136:47–62.

Sanchez HA, Villone K, Srinivas M, et al. The D50N mutation and syndromic deafness: altered Cx26 hemichannel properties caused by effects on the pore and intersubunit interactions. J Gen Physiol 2013;142:3–22.

Spray DC, Harris AL, Bennett MV. Equilibrium properties of a voltage-dependent junctional conductance. J Gen Physiol 1981;77:77–93.

Stong BC, Chang Q, Ahmad S, et al. A novel mechanism for connexin 26 mutation linked deafness: cell death caused by leaky gap junction hemichannels. Laryngoscope 2006;116:2205–10.

Thomas T, Telford D, Laird DW. Functional domain mapping and selective trans-dominant effects exhibited by Cx26 disease-causing mutations. J Biol Chem 2004;279:19157–68.

Turner DL, Weintraub H. Expression of achaete-scute homolog 3 in *Xenopus* embryos converts ectodermal cells to a neural fate. Genes Dev 1994;8:1434–47.

Valiunas V, Gemel J, Brink PR, et al. Gap junction channels formed by coexpressed connexin40 and connexin43. Am J Physiol Heart Circ Physiol 2001;281:H1675–89.

van Steensel MA. Gap junction diseases of the skin. Am J Med Genet C Semin Med Genet 2004;131C:12–9.

Veenstra RD. Size and selectivity of gap junction channels formed from different connexins. J Bioenerg Biomembr 1996;28:327–37.

Wang H, Cao X, Lin Z, et al. Exome sequencing reveals mutation in GJA1 as a cause of keratoderma-hypotrichosis-leukonychia totalis syndrome. Hum Mol Genet 2015;24:243–50.

White TW, Bruzzone R, Goodenough DA, et al. Mouse Cx50, a functional member of the connexin family of gap junction proteins, is the lens fiber protein MP70. Mol Biol Cell 1992;3:711–20.

White TW, Bruzzone R, Wolfram S, et al. Selective interactions among the multiple connexin proteins expressed in the vertebrate lens: the second extracellular domain is a determinant of compatibility between connexins. J Cell Biol 1994;125:879–92.

White TW, Deans MR, O'Brien J, et al. Functional characteristics of skate connexin35, a member of the gamma subfamily of connexins expressed in the vertebrate retina. Eur J Neurosci 1999;11:1883–90.

Wiszniewski L, Limat A, Saurat JH, et al. Differential expression of connexins during stratification of human keratinocytes. J Invest Dermatol 2000;115:278–85.

Yum SW, Zhang J, Scherer SS. Dominant connexin26 mutants associated with human hearing loss have trans-dominant effects on connexin30. Neurobiol Dis 2010;38:226–36.

Yum SW, Zhang J, Valiunas V, et al. Human connexin26 and connexin30 form functional heteromeric and heterotypic channels. Am J Physiol Cell Physiol 2007;293:C1032–48.

Zelante L, Gasparini P, Estivill X, et al. Connexin26 mutations associated with the most common form of non-syndromic neurosensory autosomal recessive deafness (DFNB1) in Mediterraneans. Hum Mol Genet 1997;6:1605–9.

Zhao HB, Kikuchi T, Ngezahayo A, et al. Gap junctions and cochlear homeostasis. J Membr Biol 2006;209:177–86.